

Design and Evaluation of RFID Deployments in a Trauma Resuscitation Bay

Siddika Parlak, *Member, IEEE*, Shriniwas Ayyer, Ying Yu Liu, and Ivan Marsic, *Member, IEEE*

Abstract—We examined configuring a radio frequency identification (RFID) equipment for the best object use detection in a trauma bay. Unlike prior work on RFID, we 1) optimized the accuracy of object use detection rather than just object detection; and 2) quantitatively assessed antenna placement while addressing issues specific to tag placement likely to occur in a trauma bay. Our design started with an analysis of the environment requirements and constraints. We designed several antenna setups with different number of components (RFID tags or antennas) and their orientations. Setups were evaluated under scenarios simulating a dynamic medical setting. We used three metrics with increasing complexity and bias: read rate, received signal strength indication distribution distance, and target application performance. Our experiments showed that antennas above the regions with high object density are most suitable for detecting object use. We explored tagging strategies for challenging objects so that sufficient readout rates are obtained for computing evaluation metrics. Among the metrics, distribution distance was correlated with target application performance, and also less biased and simpler to calculate, which made it an excellent metric for context-aware applications. We present experimental results obtained in the real trauma bay to validate our findings.

Index Terms—Object use detection, RFID, setup evaluation.

I. INTRODUCTION

PASSIVE radio frequency identification (RFID) is becoming a leading automatic identification and sensing technology. Compared to other passive systems, RFID provides faster and simultaneous detection of multiple items, longer read-range, and no-line-of-sight operability. These features support context-aware applications with item-level tagging of small and inexpensive objects.

The number and positioning of sensing components (setup design) are determined based on application requirements and constraints. Compared to other sensors, passive RFID has two features that require further consideration [1]. First, an RFID

system has two components—tags on objects and tag readers, requiring consideration of both during deployment. Second, passive RFID signal reception is sensitive to orientation of tags to antennas, as well as to interference caused by objects and people. Redundant tags and antennas are often introduced for improved performance [1]. Previous methods for configuring RFID components focused on maximizing read rates [1]–[3]. In applications that infer higher level information (e.g., motion or use detection) [4], read rate is not adequate, and target application accuracy is a more informative metric. To quantify the application's accuracy, the application must be developed, and the accuracy is affected by the performance of its software components (feature extractors and classifiers in a machine-learning strategy). For these applications, current practices include placing antennas in a grid based on intuition rather than experiments [4], [5], performing experiments to find the best placement, or using various antenna orientations and judging their usefulness from the observed results [6]. To our knowledge, existing methods do not provide a quantitative evaluation metric for the quality of the antenna placement.

We developed methods for designing and quantitatively evaluating RFID setups for high-level information inference (object use detection). Compared to prior work [2], [3], we focused on antenna deployment and jointly addressed tagging issues. To evaluate setups, we used the distance of statistical distributions of received signal strength indication (RSSI) data.

We demonstrated our setup design and evaluation using our target application of object use detection during trauma resuscitation—the initial evaluation and treatment of severely injured patients. Medical tasks, in general, can be recognized by detecting the use of objects with RFID tags attached on them [7], [8]. A trauma resuscitation environment, however, poses challenges for RFID-based detection of object use and requires careful consideration of tags and antennas placement. We first evaluated our methods in the controlled laboratory environment and then confirmed these findings using a dataset recorded in a real trauma resuscitation setting.

II. ANTENNA SETUP DESIGN AND EVALUATION

To identify optimal placement of RFID antennas for object use detection during trauma resuscitation, we simulated the resuscitation setting in our laboratory. We used Alien Technology RFID readers (ALR-9900), operating at 915 MHz that provided both the RSSI and binary detection. We used circularly polarized antennas (ALR-9611-CR, 3 dB beam width of 65°) to reduce the effect of orientation on read rate. RFID tags came from several vendors in varied size and shape.

Manuscript received November 18, 2012; revised March 20, 2013 and August 10, 2013; accepted September 13, 2013. Date of publication September 25, 2013; date of current version May 1, 2014. This work was supported by the National Science Foundation under Grant 0803732. The Editor coordinating the review process was Y. Zhang.

S. Parlak is with Qualcomm Technologies, Inc., Santa Clara, CA 95051 USA (e-mail: siddikap@qi.qualcomm.com).

S. Ayyer is with the Blackrock Financial Management, Portfolio Analytics Group, New York, NY 10022 USA (e-mail: shriniwasayyer14@gmail.com).

Y.Y. Liu is with the Department of Electrical Engineering, Purdue University, West Lafayette, IN 47904 USA (e-mail: liu282@purdue.edu).

I. Marsic is with the Department of Electrical and Computer Engineering, Rutgers University, Piscataway, NJ 08854 USA (e-mail: marsic@rutgers.edu).

Color versions of one or more of the figures in this paper are available online at <http://ieeexplore.ieee.org>.

Digital Object Identifier 10.1109/JBHI.2013.2283506

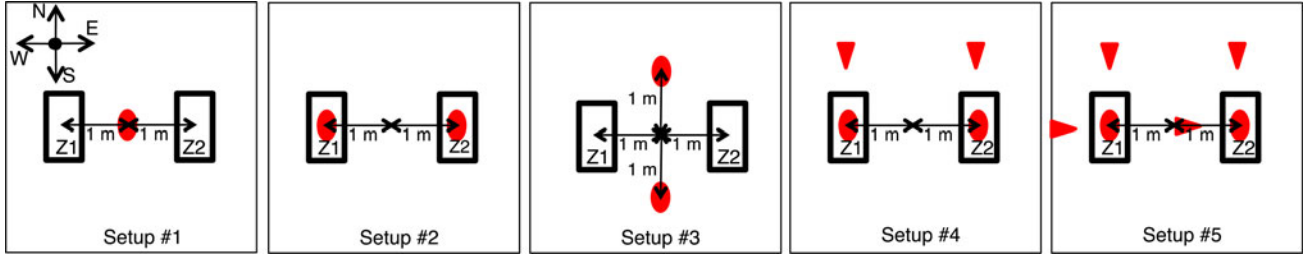


Fig. 1. Top view of five different antenna setups. Z1 represents the patient-bed zone and Z2 represents the left storage zone (see Fig. 5). Ceiling-mounted antennas are shown as ovals; angled antennas are shown as triangles.

A. Antenna Setup Design

To design our setup, we first analyzed spatial distribution of medical objects, people positioning, and object manipulation styles in the actual resuscitation environment [8].

1) *Observational Analysis*: We identified five zones where medical objects appear during resuscitations: patient-bed zone, right and left zones, and foot and head zones. Objects are stored (or left idle) in left, right, head, and foot zones; they also move between zones when relocated for use. Care providers stand or walk in the area between side zones and the patient-bed zone.

2) *Design Requirements and Constraints*: Based on our observational analysis, we identified five requirements for positioning antennas. First, cover each zone by ≥ 1 antenna. The outside areas do not require coverage due to low concentration of objects during work. Second, minimize the number of antennas to reduce the cost and radio interference. Third, place antennas to minimize interference from the human presence. Fourth, place antennas to reduce the effect of object orientation on signal reception. Finally, antennas should not hinder task performance.

3) *Candidate Antenna Setups*: During resuscitation, objects appear either on the patient bed or in the storage. We designed a prototype setting in our laboratory with two zones: the patient-bed zone (usage area, Z1 in Fig. 1) and the left zone (storage area, Z2 in Fig. 1). Each zone contained a 0.9-m tall cart. The carts were separated from 0.8 to 2.3 m, depending on the scenario. The target object was simulated by an RFID tagged rectangular cardboard box and manipulated by the experimenter.

Our baseline setup (Setup #1 in Fig. 1) included a single floor-facing, ceiling-mounted antenna, located between the two zones at 2.7 m above the floor. Based on the vendor information, we made a conic beam approximation for the directional radiation pattern with a 3 dB beam width of 65° . The resulting coverage area was a circle of radius 1.5 m at the height of the carts. The coverage area included both storage and usage zones, meeting the coverage requirement.

Setups #2 and #3 included two ceiling antennas with different viewpoints to obtain diverse information from tags. In Setups #4 and #5, we increased the number of antennas per zone to 2 and 3, respectively. We mounted new antennas on the sidewalls so they could transmit in different directions (ideally perpendicular) relative to the ceiling antennas. These new antennas were placed at 2 m height to minimize human interference. To cover the experimental area, we also slanted the antennas 60° to the floor (see Fig. 1).

B. Antenna Setup Evaluation

1) *Evaluation Metrics*: We used three criteria to measure the quality of a setup.

- 1) *Read rate*: Detecting object use required great amount of data from each tag for reliable results. We defined read rate as the *number of responses from a tag per unit of time*. Read rate is simple to calculate and provides the basic information about the quality of a deployment. Most prior work evaluated RFID performance in terms of read rate [1]–[3].
- 2) *Distribution distance of RSSI data*: High read rates are necessary but may not suffice for inferring object use since readouts only imply tag's visibility to the antennas. Object use, however, produces "fingerprints" in the RSSI sequence. For example, a blood pressure cuff is in use if it is located around the patient's arm. The fingerprints of object location and motion are important cues for object use [8]; they can be extracted from the RSSI sequence as different states of tag location and motion generate different RSSI patterns. Therefore, a preferable deployment accentuates the difference of RSSI patterns across different states.

We quantified the difference between the statistical distributions of RSSI values using the Mahalanobis distance, a similarity measure of a vector and a set of vectors representing a distribution. Unlike the Euclidean distance, it accounts for correlations among the variables. This is useful for passive RFID deployments since antennas scanning the same or overlapping regions (for reliability by redundancy) may generate correlated RSSI values, violating the independence assumption of the Euclidean distance. Also, the Mahalanobis distance is scale invariant (if variables are multiplied by a common factor), and thus independent of the RSSI magnitude. We defined our Mahalanobis-based metric to maximize the separation between different tag states (*moving or still*) [9]. Mahalanobis distance of two distributions is closely related to separability of classes in classification problems: as the average interclass distance grows and the average intraclass distance falls, classification performance should improve.

Compared to read rate, distribution distance is a more complex measure as it requires selecting a distance metric and makes assumptions on the data (e.g. normally distributed), both of which may bias the assessment of an RFID setup.

3) *Target application accuracy*: The accuracy of use detection is measured by the similarity of the hypothesis to ground truth. Several metrics can be used: precision, F-score, and classification accuracy [10]. We approximated our goal of object use detection with two cues: zone-based location and motion status [8]. We formulated both cues as classification problems and used the classification accuracy as our metric. Accuracy measures the quality of RFID setup relative to a target application, which makes it the most informative metric toward the end goal. But, unlike read rate and distribution distance, accuracy calculation requires building the application modules (feature extraction and classification), and the results may be biased by the selection of these modules.

2) *Experimental Procedure and Scenarios*: Coarse-grained location and mobility status of an object signal its usage [8]. In the trauma bay, objects moving in the patient-bed zone are more likely to be in use. Our experiments separately simulated the location and motion state changes during object use. To simulate *location change*, the tagged object stood in Z1 for 10 s, then moved from Z1 to Z2 and stood in Z2 for another 10 s. We chose the 10 s interval based on our observations of trauma teamwork: when in use, objects were manipulated for ≥ 10 s [8]. For *motion state change*, the object stood still for the first 10 s and then the experimenter manipulated and rotated the object in 3-D for another 10 s.

We designed six experimental scenarios with subscenarios simulating the characteristics of the trauma bay that may affect propagation of RFID radio signals. If a setup did not perform well under several scenarios, we omitted it from the remaining scenarios (Scenarios #2d, #5, and #6). Each scenario was repeated five times, yielding a total of 410 recordings.

- 1) *Scenario #1: Stationary environment*: The baseline scenario with no environmental factors.
- 2) *Scenario #2: Deviations in zone locations*: Although coarse-level zone locations are fixed (e.g., cabinets), the patient bed and carts may slightly move during resuscitation. To simulate these deviations, we moved the zones (i.e., carts) as follows: 2a) Z1 and Z2 moved 0.6 m north; 2b) Z1 moved 0.6 m north, Z2 moved 0.6 m south; 2c) Z1 moved 0.6 m east, Z2 moved 0.6 m west; 2d) Z1 and Z2 were lowered by 0.3 m.
- 3) *Scenario #3: Changes in object orientation*: Object tags by default faced the ceiling. To simulate random orientations, we rotated the object so that the tag 3a) faced the north wall; and 3b) faced the west wall. We did not experiment with south and east directions because tag orientation to the antennas is the same for north/south, as well as for east/west.
- 4) *Scenario #4: Changes in providers' mobility*: Providers' movement was simulated as: 4a) two people independently walked at ≈ 1 m/s; and 4b) five people walked similarly.
- 5) *Scenario #5: Multiple tags in the environment*: In addition to the target tagged object, we placed four tags in Z1 and six tags in Z2 (representing objects in storage versus use). The new tags were scattered uniformly separated about 8 cm.

6) *Scenario #6: Multiple tags and people movement*: Scenarios #4b and #5 were combined to observe the joint effect of multiple tags and providers' movement.

3) *Evaluation Methods*: To evaluate the efficiency of an antenna setup in a scenario, we calculated the average read rate, distribution distance, and application accuracy over five runs. We calculated the distribution distance between the first and second 10-s intervals of an RSSI recording session (state changed at the 10th second). For setups with multiple antennas, a corresponding vector was formed. If no data were received from an antenna, it meant that 1) the tag was too far away; or 2) the tag was within the coverage but could not be detected due to its orientation or occlusion. These possibilities were modeled by generating Gaussian-distributed values with a low mean (lower than the smallest RSSI value observed) to fill in the missing values.

We calculated the zone-based localization accuracy for location experiments and motion classification accuracy for motion experiments. Localization used binary classification to decide where the object was (in Z1 or Z2). We used a sliding-window method to map the RSSI data to a set of features. Window size of 5 s and a shift size of 2 s were selected as a compromise between accuracy (longer windows provide more accurate results) and agility (shorter windows work better for dynamic environments). Our feature vector contained the RSSI means of data received by each antenna. At each time instant, a zone-based classification module assigned one label to each feature vector. We applied different classifiers (decision trees, hidden Markov models, random forests, and support vector machines) to explore the effect of classifier selection. For motion experiments, binary classification decided whether the object was standing still or in motion. We used the same sliding window, but with RSSI standard deviations as features.

4) *Evaluation Results*: In the location experiments, we observed slight changes in read rates across setups [see Fig. 2(a)]. The highest rates resulted in Setup #1 (~ 30 reads/s). In Setups #2 and #3, the rates dropped (~ 23 reads/s) as both antennas were connected to the same reader and scanned the area in a round-robin fashion. In Setups #4 and #5, rates slightly increased with detection of tags in different orientations (~ 25 reads/s). Compared to Setup #4, the rate in Setup #5 was consistent across scenarios, indicating its robustness to environmental changes. The rates sharply fell with multiple tags (Scenarios #5, #6) due to the contention for the wireless medium using the ALOHA protocol (6 reads/s in Setup #2). Setup #5 was superior, with rates up to 13 reads/s.

Mahalanobis distance increased with more antennas [see Fig. 2(b)]. Lowest scores were obtained in Setup #1 with a single antenna. For Setups #2 and #3 (with two antennas), Setup #3 had lower distribution distance as the two object locations were symmetric to antennas' propagation pattern, resulting in similar RSSI patterns. Setup #5 had the greatest distribution distance for it had the most antennas, followed by Setups #4 and #2 with four and two antennas, respectively. Both KL (not shown due to space limitation) and Mahalanobis distance yielded similar rankings of setups, indicating that our results are independent of the distribution distance measure type. The best results were

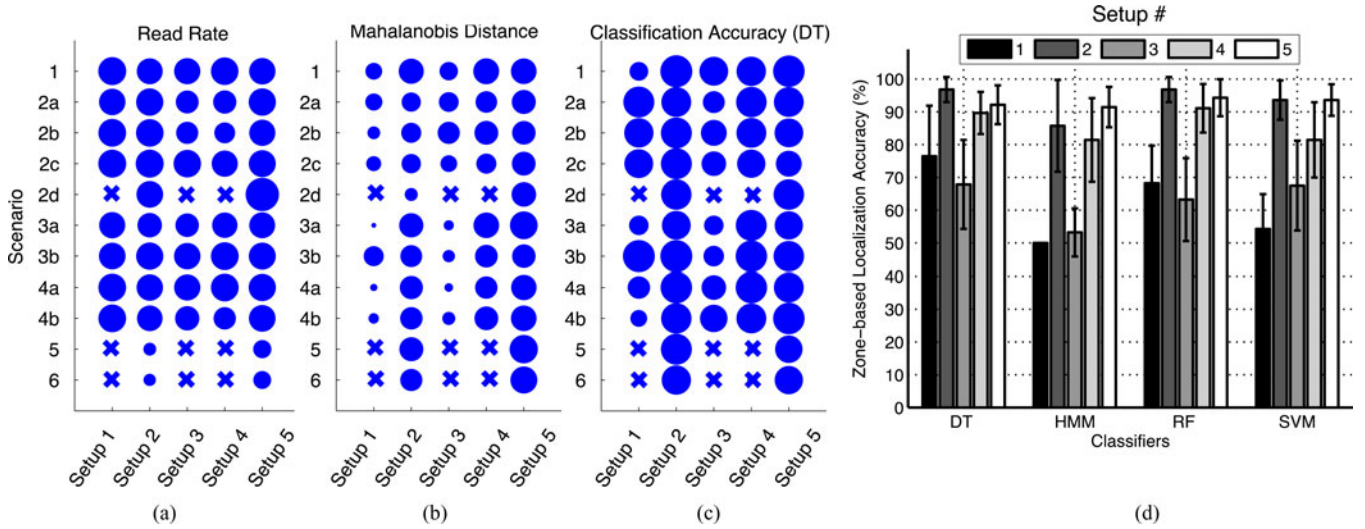


Fig. 2. Experimental results for *location state change*. (a) Read rate. (b) Mahalanobis distance on logarithmic scale. (c) Classification accuracy with decision trees. (d) Average classification accuracy for different setups obtained with different classifiers. Scenarios #2d, #5, and #6 were simulated only for Setups #2 and #5, which performed the best in the other scenarios.

achieved with at least one ceiling-mounted, floor-facing antenna per zone (see Fig. 2). Adding more antennas increases the sensitivity of radio signals to different object states, but may reduce the readout rate and hence the quality of input data for distribution distance calculation.

Setups #2, #4, and #5 provided the best zone-based localization for all scenarios [see Fig. 2(c)]. For these setups, the variation across scenarios was hardly noticeable. In contrast, classification accuracy significantly varied by the scenario for Setups #1 and #3. Other classifiers produced similar setup rankings [see Fig. 2(d)]. Comparing the best performers, Setup #5 was always slightly better than Setup #4, but sometimes worse than Setup #2 with only two antennas [see Fig. 2(d)]. With more antennas, the diversity of reception increased, as did the interference between antennas. The side antennas were more susceptible to interference caused by human motion. These results justify the importance of ceiling-mounted antennas: setups with a centrally placed ceiling antenna (Setups #2, #4, and #5) outperformed other setups.

Distribution distance increased with more antennas. However, after a certain distribution distance was exceeded, localization and motion detection accuracy saturated. We identified a linear correlation between logarithm of distribution distance and classification accuracy. Therefore, if there is a limitation on the number of antennas (cost constraints), a setup decision can be made solely based on the distribution distance without developing the entire recognition system. Distribution distance was biased toward setups with more antennas, but this bias may be alleviated by applying a logarithm.

In the motion experiments, Setups #2, #4, and #5 had the best motion detection. Setup #5 was superior to #2 because it could sense different object orientations. In general, we observed lower distances and accuracy scores for recognizing motion states than for location states. We conclude that tag location changes cause greater RSSI deviations, and so are easier to detect than tag movement around the same location.

III. TAG SETUP DESIGN AND EVALUATION

Here, we address the challenges of tag placement, as tagging liquid containers and objects with narrow cylindrical surfaces. Maximizing readout rates for these objects is desirable, but not priority, as high rates do not guarantee inference of object use.

A. Tag Setup Design

1) *Observational Analysis*: Objects in the trauma bay are composed of materials such as plastic (tubes), rubber (parts of blood pressure cuff), metal (laryngoscope), and liquid (saline fluid). They may have regular or irregular shapes with narrow surfaces. Some objects are in contact with providers' hands or patient body for longer periods, which sharply reduces reception from their tags.

2) *Design Requirements and Constraints*: To achieve sufficient read rates, tags must be visible to the antennas regardless of the object orientation. Special tags should be used to tag metallic objects and liquid containers, or the contact with the object should be minimized. Tag shape should be preserved (avoid folding) so that tag antenna can function well and not hinder the object use. Tags should be placed on surfaces that are not in contact with providers' hands or body during work. The effect of human contact, however, can be exploited to infer interactions (see Section III-A3). Finally, the number of tags should be minimized to reduce the cost and message collisions during tag-reader communication.

3) *Candidate Tag Setups*: We evaluated tag placement using experimental scenarios.

1) *Scenario #1: Tag type selection and placement based on material*: RFID performs poorly on metallic objects and liquid containers. Special tags are available, but they are expensive, especially for disposable objects. Regular tags can be used for such objects if the tag minimally overlaps with the object [3]. We evaluated this approach by tagging a liquid container [see Fig. 3(a)] along its length and width.

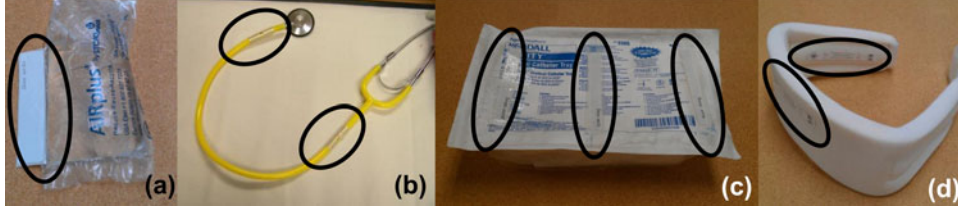


Fig. 3. Objects used in tag placement experiments. (a) Fluid bag, one tag attached along the length. (b) Stethoscope, two tags folded around the tube. (c) Foley catheter kit, three tags attached to the wrapping. (d) Cervical collar, two tags attached in tandem.

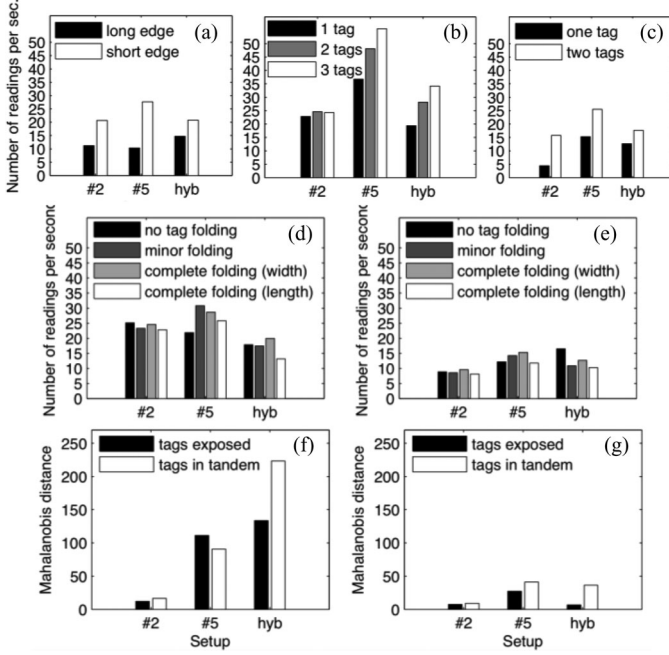


Fig. 4. Tag placement experiments. (a) Scenario #1 (fluid bag). (b) Scenario #2 (Foley cath.). (c) Scenario #2 (stethoscope). (d) Scenario #3 (Stet. on cart). (e) Scenario #3 (Stet. around neck). (f) Scenario #4 (Collar). (g) Scenario #4 (stethoscope).

- 2) *Scenario #2: Determining the number of tags:* Multiple tags are useful when a single tag has low detection rate. We used a Foley catheter kit [see Fig. 3(c)] and stethoscope [see Fig. 3(b)] to explore the benefits of multiple tags.
- 3) *Scenario #3: Tag placement based on object shape:* Most medical objects have irregular shapes, requiring different tag-placement strategies. We assessed the effect of tag folding on read rates using a stethoscope with four folding styles: tag attached along its width, no folding; minor folding; complete folding; and tag attached along its length, complete folding.
- 4) *Scenario #4: Objects are in contact with body when in use:* To exploit this cue, we attached two tags in tandem: one at a location where the tag would be covered when in use, and one where it would be exposed to RF signal. When the object was not in use, we expected strong signal from both tags; when in use, the covered tag would emit weaker or no signal. We used a collar [see Fig. 3(d)] and stethoscope.

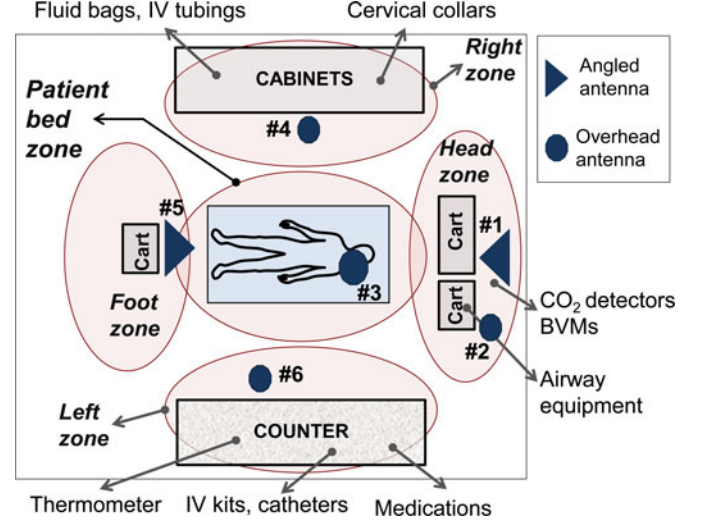


Fig. 5. Environmental setting of a trauma bay. Primary zones and storage locations of some objects are indicated.

B. Tag Setup Evaluation

1) *Tag Evaluation Using Selected Antenna Setups:* To evaluate our tag-placement strategies, we experimented in our two-zone setting (see Fig. 1). Each experiment was repeated using antenna Setups #2 and #5, which scored best in placement experiments. We also combined Setups #2 and #5 by scanning the storage zone with a ceiling antenna, and the bed zone with one ceiling- and two slanted antennas. Extra antennas were preferred for the bed zone since most object interactions occurred in this zone.

We ran 57 experimental sessions, each repeated five times, for a total of 285 sessions. Each session had a 20-s RSSI recording, with the object state changing at the 10th second. For Scenarios #1, #2, and #3, we collected data in both zones to eliminate zone-specific effects (e.g., number of antennas).

2) *Evaluation Metrics and Methods:* We used the read rate as the metric in Scenarios #1, #2, and #3 since the number of readings from an object must suffice for computing the distribution distance and classification accuracy with high confidence. Our main statistic for distance and classification was the RSSI mean. Assuming a normal distribution, we needed a sample size of $n = 4\sigma^2/M^2$ for 95% confidence that the sample mean was within the distance M of the true mean. Our initial analysis of the RSSI data showed that $M \geq \sigma/4$ was needed for distinguishing the patient-bed and storage zones, corresponding to 64

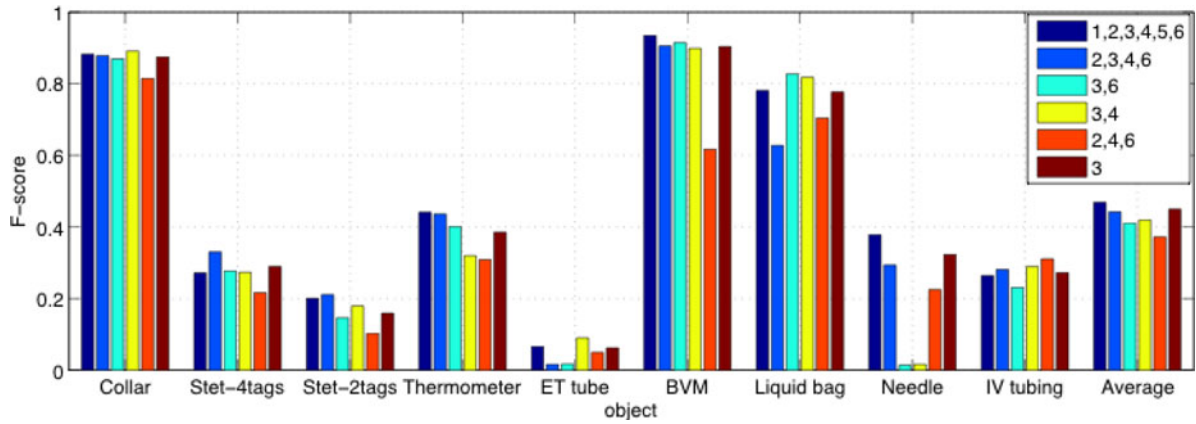


Fig. 6. F-scores for detecting use of several object types using different sets of antennas (indicated in the legend).

samples. We set threshold at 64 readouts per decision window. Given our window length of 5 s, we needed at least 13 reads/s. Since Scenario #4 was related to the information about object use, we used the metrics of distribution distance and classification accuracy.

3) *Evaluation Results:* We found that sufficient read rates were obtained for a liquid container when a tag was attached along its short edge [see Fig. 4(a)], showing the feasibility of using regular tags for liquid containers when the tag is attached along its short edge.

We observed higher performance gain with multiple tags attached to irregularly shaped objects. Multiple tags always improved read rates but also increased message collisions in tag-reader communication. In our experiments, a single tag appeared to suffice for the Foley catheter kit, which has a regular shape [see Fig. 4(b)]. In contrast, read rates from the stethoscope indicated the need for more tags [see Fig. 4(c)].

For tag antennas to function, proximity to human body should be avoided. Although tolerable, tag folding reduced read rates [see Fig. 4(d)]. The impact of human proximity was harsher [see Fig. 4(e)] and two tags did not suffice for confident estimation of descriptive statistics. Tags should, therefore, be used on surfaces with low likelihood of human contact.

Because our aim was to infer object use, we used the distribution distance metric to evaluate tandem tagging. For the collar and stethoscope, our tagging strategy yielded higher distribution distance and easier use detection [see Fig. 4(f) and (g)].

IV. EXPERIMENTS IN THE TRAUMA RESUSCITATION BAY

To validate our methods in a realistic setting, we conducted a deployment study in an actual trauma center. We used a hybrid approach for antenna placement: Setup #5 for the patient bed zone (where most work occurs) and Setup #2 for other zones. This deployment had one overhead antenna per zone and two angled antennas scanning the patient bed zone (see Fig. 5). A total of 31 objects were tagged with commercial tags using our findings from the laboratory experiments.

RFID data were collected during 32 mock resuscitations performed by trauma team members for training purposes. Resuscitations lasted about 20 min each and included scenarios with injuries requiring different treatments. To establish the ground

truth, a member of our research team annotated object interactions (object ID, interaction start and end times) by watching videotaped resuscitations.

The RSSI data were processed with machine learning. We extracted statistical features and trained classifiers to detect object use events. During resuscitations, a large number of tagged objects were within antennas view, reducing read rates per object. To mitigate the effect of low number of samples, we enlarged the window from 5 to 12 s.

A. Experiments With Antenna Placement and Findings

To validate our laboratory antenna deployment findings, we selectively omitted the RSSI from some antennas and re-ran our use detection algorithm. We measured the accuracy of object use detection by F-score [10] (see Fig. 6). The setup with all six antennas scored the best (average $F = 47.3\%$), but fewer antennas yielded comparable results ($F = 44.2\%$ with antennas #2, #3, #4, #6; $F = 44.7\%$ with a single central antenna #3). In contrast, the setup without antenna #3 (above the bed) performed the worst ($F = 37.2\%$ with antennas #2, #4, #6).

These results quantified the contribution of each antenna and confirmed our laboratory findings: although object orientations varied during the work, ceiling antennas tracked objects better than sidewall antennas. In addition, the results highlighted the importance of the antenna above the patient bed, which is the main working zone. Due to the configuration of the workspace, antenna #3 alone performed comparably to the six-antenna setup. Antenna #3 alone was able to detect objects brought to the bed zone while other zones were mostly out of its coverage. As a result, object relocation to the patient bed caused a significant change in the RSSI from antenna #3. We did not observe this phenomenon in our laboratory using Setup #1 since both zones were in close proximity and covered by a single antenna. This observation confirmed our approach for placing an RFID equipment so that the received signal pattern change is maximized with the tag state change.

B. Experiments With Tag Placement and Findings

Our results showed that RFID tags worked for liquid containers. The use of fluid bags was detected with F-scores $\geq 75\%$, validating our tactic of attaching a tag along its width.

For packaged objects, a single tag usually sufficed and no special tagging instructions were needed. ET tube had the worst performance despite having two tags (see Fig. 6). This result suggests that other factors may affect use detection.

For irregularly shaped objects, multiple tagging made improvement. The tag on stethoscopes was folded along width to avoid hindering the use. We tagged one stethoscope with two and another with four tags, obtaining better F-scores for the one with four tags (see Fig. 6). This result supported our laboratory findings. The collar, BVM, and thermometer were tagged to expose at least one tag to radio signal when in use. The use of these objects was detected with relatively high F-scores.

In addition to material and shape, factors such as storage location, duration of use, and relocation time also affected use-detection rates. The use of objects stored in the left or right zones was detected with higher F-scores since they were distant from the bed. Relocation from these zones to the bed showed clearly in the RSSI sequence, compared to relocation from the head to patient bed zone. The collar and fluid bag were in use for an extended period, leading to a lower chance of a miss or confusion with other disturbances.

Tandem tagging reduced false alarms for relocation without actual use. We formulated a rule in line with our tandem tagging approach: until the signal from the tag inside the collar is completely lost, reject all usage events declared by the classifier. This approach helped when the collar stayed on the bed for a long time without being placed on the patient.

V. CONCLUSION

Our contribution is in quantifying the quality of RFID components placement. Without a well-defined metric, it was unclear how increased coverage by multiple antennas would trade off with reduction in the number of samples per antenna and interference. We found that distribution distance was more informative metric than read rate. Distribution distance was well correlated with target application performance, as well as less biased and simpler to calculate. Although object material and shape posed challenges for tagging, we were able to effectively tag fluid bags along their edge. We also observed that use detection depended on other, object-specific factors.

REFERENCES

- [1] A. Rahmati, L. Zhong, M. Hiltunen, and R. Jana, "Reliability techniques for RFID-based object tracking applications," in *Proc. IEEE/IFIP Int. Conf. Dependable Syst. Netw.*, 2007, pp. 113–118.
- [2] S. Hodges, A. Thorne, H. Mallinson, and C. Floerkemeier, "Assessing and optimizing the range of UHF RFID to enable real world pervasive computing applications," in *Pervasive Computing*, vol. 4480, A. LaMarca, M. Langheinrich, and K. Truong, Eds. New York, NY, USA: Springer, 2007, pp. 280–297.
- [3] K. M. Ramakrishnan and D. D. Deavours, "Performance benchmarks for passive UHF RFID tags," in *Proc. 13th GI/ITG Conf. Meas., Model. Eval. Comput. Commun. Syst.*, 2006, pp. 137–154.
- [4] B. Jiang, K. P. Fishkin, S. Roy, and M. Philipose, "Unobtrusive long-range detection of passive RFID tag motion," *IEEE Trans. Instrum. Meas.*, vol. 55, no. 1, pp. 187–196, Feb. 2006.
- [5] K. Kleisouris, B. Firmer, R. Howard, Y. Zhang, and R. P. Martin, "Detecting intra-room mobility with signal strength descriptors," in *Proc. ACM Int. Symp. Mobile Ad Hoc Netw. Comput.*, 2010, pp. 71–80.

- [6] E. Welbourne, K. Koscher, E. Soroush, M. Balazinska, and G. Borriello, "Longitudinal study of a building-scale RFID ecosystem," in *Proc. ACM 7th Int. Conf. Mobile Syst. Appl. Serv.*, 2009, pp. 69–82.
- [7] J. E. Bardram, A. Doryab, R. M. Jensen, P. M. Lange, and K. L. G. Nielsen, "Phase recognition during surgical procedures using embedded and body-worn sensors," in *Proc. IEEE Int. Conf. Pervasive Comput. Commun.*, 2011, pp. 45–53.
- [8] S. Parlak, A. Sarcevic, I. Marsic, and R. S. Burd, "Introducing RFID technology in dynamic and time-critical settings: Requirements and challenges," *J. Biomed. Informatics*, vol. 45, no. 5, pp. 958–974, 2012.
- [9] S. Parlak, "Object detection and activity recognition in time-critical dynamic medical settings using RFID," Ph.D. dissertation, Dept. Elect. Comp. Eng., Rutgers Univ., New Brunswick, NJ, USA, 2013.
- [10] J. A. Ward, P. Lukowicz, and H. W. Gellersen, "Performance metrics for activity recognition," *ACM Trans. Intell. Syst. Technol.*, vol. 2, no. 1, pp. 6:1–6:23, Jan. 2011.



Siddika Parlak (S'08–M'13) received the B.S. and M.S. degrees from the Department of Electrical and Electronics Engineering, Bogazici University, Istanbul, Turkey, in 2006 and 2008, respectively, and the Ph.D. degree from the Department of Electrical and Computer Engineering, Rutgers University, New Brunswick, NJ, USA, in 2013.

Her research interests include speech processing, ubiquitous computing, and context-aware systems.



Shriniwas Ayer received the B.E. degree in electronics and telecommunications engineering from the University of Mumbai, Mumbai, India, and the M.S. degree in electrical and computer engineering from Rutgers University, New Brunswick, NJ, USA.

His research interests include data analysis and machine learning.



Ying Yu Liu received the B.S. degree in electrical and computer engineering from Rutgers University, New Brunswick, NJ, USA, and is currently a graduate student in electrical and electronics engineering at Purdue University, West Lafayette, IN, USA.

His research interests include computer architecture and very large scale integration design.



Ivan Marsic (M'94) received the Dipl.Ing. and M.S. degrees in computer engineering from the University of Zagreb, Zagreb, Croatia, and the Ph.D. degree in biomedical engineering from Rutgers University, New Brunswick, NJ, USA, in 1994.

He is currently a Professor in the Department of Electrical and Computer Engineering, Rutgers University. His research interests include software engineering and sensor networks for healthcare applications.